J. Water Environ. Nanotechnol., 3(3): 243-253 Summer 2018

ORIGINAL RESEARCH PAPER

Synthesis and Application of Amin-modified Fe_3O_4@MCM-41 Core-shell Magnetic Mesoporous for Effective Removal of pb^{2+} ions from Aqueous Solutions and Optimization with Response Surface Methodology

Kamal Alizadeh*, Esmail Khaledyan, Yagoub Mansourpanah

Department of Chemistry, Lorestan University, Khorramabad, Iran

Received: 2018.05.20 Accepted: 2018.07.14 Published: 2018.07.30

ABSTRACT

In this study, a selective, fast and novel magnetic mesoporous silica sorbent Fe_3O_4@MCM-41-NH_2, was synthesized, functionalized and has been used for the removal of Pb^{+2} ions from aqueous solution. The characteristics of the Fe_3O_4@MCM-41-NH_2 sorbent was investigated by XRD, VSM, SEM, TEM, BET, and FT-IR. The response surface methodology (RSM) based on central composite design (CCD) was utilized for estimating the effects of parameters, namely contact time (min), pH, the quantity of adsorbent (g) and initial concentration of Pb^{+2}. The quadratic model was used as the best model for guessing variables. The results of the analysis of variance for this model were obtained with a high F-value (50.28), very low P-value (<0.0001) and non-significant lack of fit (0.2251). The maximum adsorption capacity was obtained at 46.08 mg/L. Fitting equilibrium data with different isotherm models shows that Freundlich isotherm was the best-fitted model. The pseudo-second-order model was the best model for fitting experimental data.

Keywords: *Adsorption, Central Composite Design, Magnetic Mesoporous Silica Sorbent, Pb^{+2}, Removal*

How to cite this article

Alizadeh K, Khaledyan E, Mansourpanah Y. Synthesis and Application of Amin-modified Fe_3O_4@MCM-41 Core-shell Magnetic Mesoporous for Effective Removal of pb^{2+} ions from Aqueous Solutions and Optimization with Response Surface Methodology. J. Water Environ. Nanotechnol., 2018; 3(3): 243-253. DOI: 10.22090/jwent.2018.03.005

INTRODUCTION

The production of waste from many industrial processes leads to environmental pollution [1]. Increasing use of heavy metals in industrial processes results in severe pollution of the environment [2]. Heavy metals are non-biodegradable, tend to bioaccumulation and are toxic at very low concentrations [3]. Lead is one of the most common heavy metals which is used extensively in many industries such as fuels, coatings, automobile, petroleum, pigments, storage and rechargeable batteries [4,5]. Lead in drinking water, even at low levels, in the long run, can cause serious health problems, including nausea, reduced alertness, the formation of kidney stones, hysteria, coma and induce an effect on metabolism [6]. In the last decade, extensive research has been done to find techniques to the removal of lead from aqueous such as chemical perception, ion exchange, adsorption, coagulation and floatation, cementation, and reverse osmosis [7-12]. Among these techniques, adsorption has been widely used due to its cost-effectiveness, flexibility, simplicity, selective and adsorbent reusability after multi-reuse cycles [13, 14]. Mesoporous silica nanoparticle (MSN) has unique properties such as high surface area, controllable particle size, high pore volume and tunable pore size. MCM-41 is one of the most sorbent widely used among the mesoporous silicate because of its

* Corresponding Author Email: *Alizadehkam@yahoo.com*
Alizadeh.k@lu.ac.ir

structural simplicity and easiness in preparation by a liquid crystal template mechanism. MCM-41 samples have a great number of silanol groups, therefore, surface modification can be done easily with organosilanes agent resulting in the increased absorption capacity [15].

Magnetic nanocomposite as an important class of nanocomposite, with magnetite core which is able to simply separated from the solution by using external magnate and mesoporous silica shells, have attracted increased attention recently [16]. The ultimate plan of this research is to make an adsorbent for the effective and rapid elimination of Pb^{+2} ions from wastewater samples. For this point, a core-shell magnetic Fe_3O_4@MCM-41 nanocomposite was synthesized with a surfactant-directed sol-gel method. After that, the surface of the magnetic core-shell nanocomposite was modified by 3-aminopropyltriethoxysilane (APTES). The effect of a variety of conditions on the removal of lead ions has been investigated with a central composite design (CCD) under response surface methodology (RSM).

EXPERIMENTAL

Reagents and Materials

Cetyltrimethylammonium bromide (CTAB), 3-aminopropyltriethoxysilane (APTES), and tetraethyl orthosilicate (TEOS) were purchased from Sigma–Aldrich. Other materials were analytically graded and were used as received without further purification.

Instruments

Atomic absorption spectrometer (Shimadzu model AA 880, Japan) was used to determine lead at 283.3 nm. Scanning Electron Microscope (SEM) model FE-SEM from TESCAN Company was applied for the morphological structure of nanocomposite. Transmission Electron Microscopy (TEM) images were obtained by a Zeiss-EM10C electron microscope (Germany) at an accelerated voltage of 80 kV. FT-IR spectrum was recorded on a Shimadzu FT-IR spectrometer model 8400S (Japan). XRD patterns were obtained by X-ray diffractometer (Perkin Elmer). A measurement of the specific surface area has been made by nitrogen adsorption P/P0 = 0.995, at 77 ˚K using a Brunauer-Emmett-Teller (BET) surface analyzer, Belsorp-Mini II, Bel Japan, Inc., (Osaka, Japan). The magnetic properties of Fe_3O_4@MCM-41 and Fe_3O_4@MCM-41-NH_2 were measured with a Vibrating sample magnetometer (VSM, MDKB, Daghigh Meghnati kavir Co., Iran).

Preparation of magnetite nanocomposite

Coprecipitation method, which is common and sufficient for synthesis magnetic nanoparticle has been used for preparing magnetic nanoparticles [17]. Briefly, 25 mmol of iron(II) chloride tetrahydrate, 25 mmol of iron(III)chloride hexahydrate and 150 ml of deionized water were placed in a three-neck flask. This mixture was heated at 60 ^{0}C for about 4 h. To prepare the Fe_3O_4@MCM-41 with stöber method [18], 0.50 g of the Fe_3O_4 nanoparticle were placed in a beaker, 120 ml deionized water and 60 ml ethanol was added and the system was homogenized by ultrasonication for 30 min. Then 1.2 ml of ammonium hydroxide (25%) was added slowly under N_2 flow, the color of the solution turns rapidly to dark. Total mixture was stirred for 1h at room temperature, then 10 ml of CTAB solution (10 M) was added dropwise under vigorous stirring for 1 h followed by adding TEOS (1.05 g) slowly and allowed to stir for 24 h. Finally, the resulting products were collected using external magnetic and thoroughly washed with ethanol/distilled water and dried in a vacuum oven at 60 ^{0}C for 24 h. The magnetic nanocomposite was calcined to remove the surfactant completely. This procedure was performed under a thermal ramp of 1 ^{0}C/min to 550 ^{0}C and then held at 550 ^{0}C for 6 h in air atmospheric. For modifying the magnetic nanocomposite with APTES, 1 g of magnetic nanocomposite and 6 ml of APTES were dispersed in anhydrous toluene and the mixture was kept in reflux condition at 40 ^{0}C for 4 h under N_2 atmosphere. After that, the modified magnetic nanocomposite was collected by an external magnetic and washed with ethanol and dried under ambient condition for 24 h [19].

Batch adsorption of Pb^{+2}

The adsorption experiments were performed in the batch mode under constant stirring of 150 rpm at room temperature. Each experiment was done in Erlenmeyer. To investigating the adsorption isotherms desired amount of adsorbent Fe_3O_4@MCM-41-NH_2 was added into 25 ml solution of lead ions with a concentration of 4-24 mg/l in natural pH and mechanical stirring at 150 rpm for 5 min to reach equilibrium at room temperature. The pH system was adjusted by the addition of NaOH (0.1M) or HCl (0.1M). The adsorbent was

separated from the solution by applying an external magnet bar placed outside Erlenmeyer. The residual concentrations of lead ions in the solution were determined by flame atomic absorption spectrophotometer (FAAS). The amount of Pb^{+2} uptake per gram of magnetic nanocomposite at equilibrium was calculated from the following equation:

$$q_e = \frac{C_0 - C_e}{m} \times V \quad (1)$$

Where C_0 and C_e are initial concentration and the equilibrium concentration of lead ions in solution and m (g) is the mass of adsorbent and V (L) is the volume of the solution.

Desorption

Desorption studies were carried out with a 0.01M solution of HCl as eluent. After the collecting adsorbent by an external magnetic, It was stripped using 5 ml of HCl at 25 ^{0}C for 5 min. Whereas Lead adsorption is highly pH related, in acidic condition so H^+ competes for coordination by first amino groups on the surface of the nanoparticle. Therefore, H^+ could be exchanged with coordinated metals ions and released them. The reuse desorption was elevated in five continuous adsorption and desorption cycles. The results showed that the adsorbent can be used and regenerated several times without any decrease in its efficiency after adsorption and eluted with HCl 0.01M. Schematic design of the proposed process is represented in Scheme 1.

RESULTS AND DISCUSSION

Characterization of Fe_3O_4@MCM-41-NH_2

As previously reported in our research group, the synthesized core-shell magnetic Fe_3O_4@MCM-41-NH_2 was firstly examined by the XRD analyses, SEM, and TEM techniques, and it can be accessible in the corresponding article [19].

Additionally, a nitrogen isothermal adsorption technique was employed in order to investigate the textural property and pore structure of the

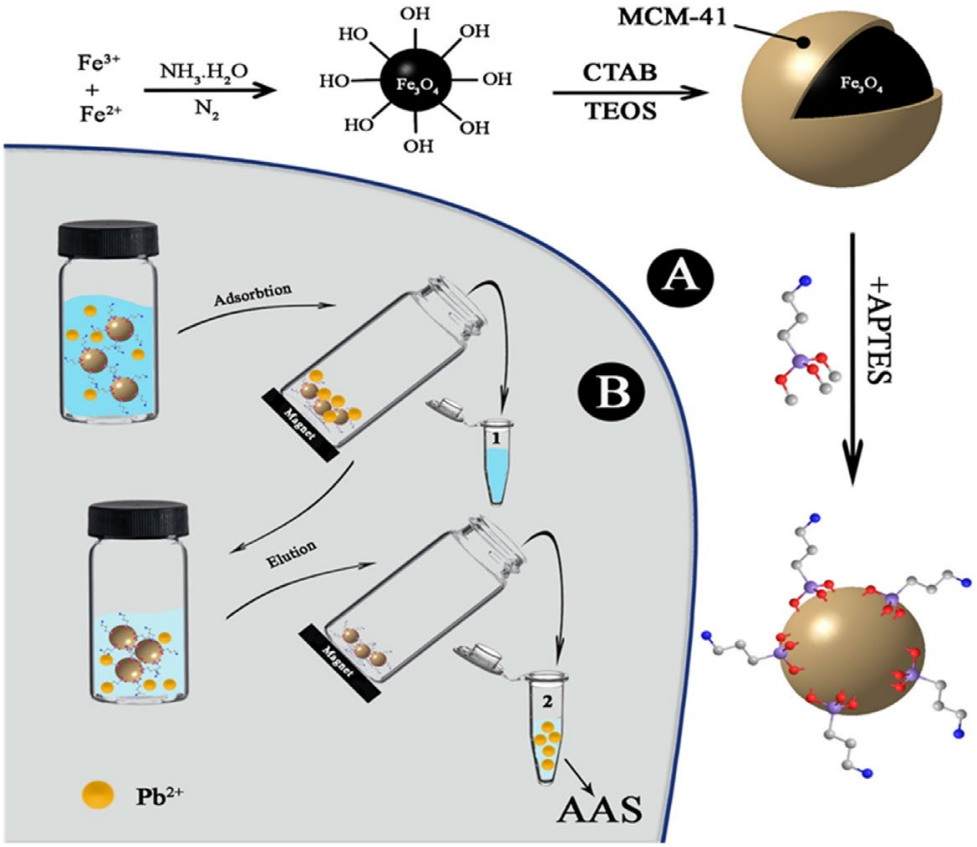

Scheme 1. Employed schematic experiment for the rapid removal of Pb^{2+} from environmental wastewater samples using a core-shell magnetic Fe_3O_4@MCM-41-NH_2 modified by 3-aminopropyltriethoxysilane.

modified magnetic nanocomposite, Fe_3O_4@MCM-41-NH_2. The information in Table 1 represents the N2 adsorption-desorption isotherm and pore size distribution of nanocomposite. Based on BJH theory, the analysis of BET show as the mean surface area of our composite was 162.27 m2/g and total pore volume 0.1114 cm^3/g with a pore size of 2.7458 nm, thus it belongs to a mesoporous category.

The functional groups in the synthesized Fe_3O_4, Fe_3O_4@MCM-41 and Fe_3O_4@MCM-41-NH_2 were recognized by FT-IR analysis. The FT-IR spectrum of Fe_3O_4@MCM-41 (Fig. 1b) can confirm the formation of mesoporous shell on the surface nanomagnetic Fe_3O_4 (Fig. 1a). As can be seen in this figure three peaks at 790, 960, 1080 were assigned to vibration of Si-OH, symmetric and asymmetric stretching of SiOSi bond respectively. Also, the FT-IR spectrum of the magnetic nanocomposite supports 3-aminopropyltriethoxysilane (APTES) loading onto the Fe_3O_4@MCM-41. The amine functionalization of Fe_3O_4@MCM-41 with APTES will make two extra absorption peak at 1618 and 2931cm^{-1} (Fig. 1c) that is related to -CH_2 stretching and bending vibration of N-H bond respectively [19]. In addition, a broadband at 3400–3600 cm^{-1} in nanocomposite can be attributed to the stretching vibration of N–H group in APTES. Most of these bands disappeared in the synthesized amino-functionalized nanocomposite, with adsorbed Pb(II) on it as given a picture in Fig. 1d, indicating an obvious difference with unadsorbed nanocomposite.

The magnetization curves of the Fe_3O_4@MCM-41 and Fe_3O_4@MCM-41@NH_2 nanocomposite recorded with VSM in room temperature are shown in Fig. 2. The saturation magnetization for Fe_3O_4@MCM-41 and Fe_3O_4@MCM-41@NH_2 are 27.75 and 22.52 emu/g respectively. A little decrease in magnetic saturation could be due to the 3-aminopropyltriethoxysilane shell coated on the magnetic particles.

Table 1. BET specific surface area, average pore diameter and total pore volume of the magnetic nanocomposite Fe_3O_4@MCM-41-NH_2.

V_m	37.281 [cm^3(STP) g^{-1}]
$a_{s,\ BET}$	162.27 [m^2 g^{-1}]
C	389.75
Total pore volume (p/p_0=0.990)	0.1114 [cm^3 g^{-1}]
Average pore diameter	2.7458 [nm]

Response Surface Methodology (RSM)

One of the most general experimental design is the Response Surface Methodology based on Central Composite Design (CCD). This method is a useful mathematical and statistical techniques that employed to study the main effects factors and the interaction among factors and also determine the optimum value of each factor [20]. The main factors are pH, initial lead concentration(mg/L), magnetic nanocomposite dosage(g) and time contact (min) and their levels are shown in Table 2. CCD was designed to investigate the effects of factors on percent recovery (%)(Table 3).

The mathematical relationship between dependent variable and independent variables was approximated by the following quadratic model:

$$y = \beta_0 + \sum_{i=1}^{k} \beta_i x_i + \sum_{i=1}^{k} \beta_{ii} x_i^2 + \sum_{i} \sum_{j=i+1} \beta_{ij} x_i x_j \quad (2)$$

Where y is the percent removal, β_0 is constant,

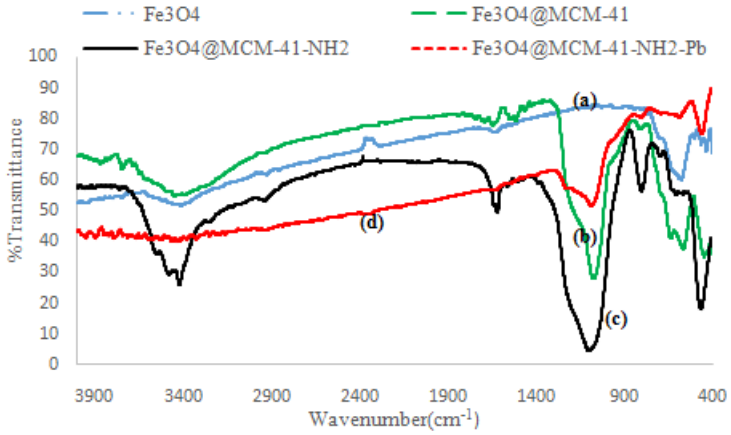

Fig. 1. FT-IR spectra of synthesis nanomagnetic

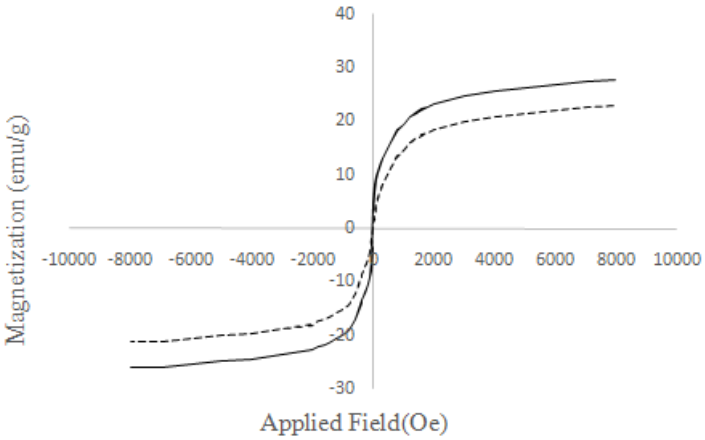

Fig. 2. Magnetic curves of the (____) Fe_3O_4@MCM-41 and (……) Fe_3O_4@MCM-41@NH_2

Table 2. Independent variables and and their coded levels

Symbol	Variables	Low(-α)	-1	+1	High(+α)	Unit
A	pH	3	4.5	7.5	9	-
B	M adsorbent	0.001	0.0045	0.0115	0.015	g
C	Stirrer time	1	2	4	5	min
D	Pb^{+2} Concentration	5	15	35	45	ppm

Table 3. Design matrix for the CCD

Run	pH	M adsorbent	C_{Pb}^{+2}	time	R%	Run	pH	M adsorbent	C_{Pb}^{+2}	time	R%
1	6	0.0080	25	3	90.34	16	4.5	0.0115	35	2	78.74
2	4.5	0.0045	35	2	74.82	17	7.5	0.0045	15	2	77.32
3	7.5	0.0115	35	2	84.84	18	6	0.0080	25	3	89.40
4	7.5	0.0115	15	2	88.71	19	7.5	0.0115	35	4	92.51
5	4.5	0.0045	15	2	76.549	20	6	0.0080	25	3	90.73
6	4.5	0.0115	15	4	92.38	21	6	0.0150	25	3	94.82
7	9	0.0080	25	3	81.67	22	6	0.0080	25	3	90.83
8	7.5	0.0045	35	2	80.81	23	6	0.0080	25	3	90.72
9	4.5	0.0045	15	4	80.82	24	4.5	0.0115	15	2	90.41
10	6	0.0080	5	3	88.83	25	6	0.0080	25	1	82.35
11	7.5	0.0115	15	4	91.29	26	6	0.0080	25	5	94.29
12	6	0.0010	25	3	75.07	27	3	0.0080	25	3	73.96
13	7.5	0.0045	15	4	80.41	28	6	0.0080	25	3	92.46
14	4.5	0.0045	35	4	81.58	29	7.5	0.0045	35	4	87.71
15	4.5	0.0115	35	4	82.51	30	6	0.0080	45	3	82.05

β_i, β_{ii} and β_{ij} are regression coefficients and χ_i and χ_j denoted dependent variables.

Response surface optimization: ANOVA result

The results of the analysis of variance (ANOVA), which is used to evaluate the model from the Design expert software are listed in Table 4, According to the results of 30 experiments a quadratic regression model is suitable to describe the removal percent:

$$\text{Removal}(\%)Y=90.75+1.72\times A+4.20\times B-1.16\times C+2.54\times D+0.051\times AB+1.92\times AC+0.22\times AD-2.13\times BC-0.31\times BD+0.82\times CD-3.28\times A^2-1.50\times B^2-1.38\times C^2-0.66\times D^2 \quad (3)$$

where Y is the lead removal response, A, B, C, and D are the coded values of the variables including the initial solution pH (A), the mass of adsorbent (B), contact time (C), and the initial lead ion

concentration (D) respectively. The significance of each term was determined by the P-values and the F-values. The smaller the P-value and the larger the F-value, the more significant is the corresponding term. In this study, it was found that the regression between the response and independent variables was statistically significant at the F-value of 50.28 implies the model is significant. There is only a 0.01% chance that an F- value this larger could occur due to noise. The predicted R-Squared of 0.8976 is in a reasonable agreement with the adjusted R-Squared of 0.9597; i.e. the difference is less than 0.2. Adequate precision indicates the ratio of the signal to the noise is greater than 4 that would be desirable. Thus, the Adeq. the precision of 21.457 shows an adequate signal.

To understand the interaction between variables, 3D response surface plots were used. Fig. 3 shows the interaction between two interacting parameters when the other parameters were kept at fixed levels using the constructed models by Design-Expert software. It is noticeable that the pH is an effective variable in the adsorption and removal of Pb^{+2} because by changing the pH, the media of solution and sites on the surface of adsorbent could be changed. As can be seen in the Fig (3A-C), maximum removal of Pb^{2+} can be observed at pH of about 6.5-7.5. We suppose that the binding mechanism of Pb^{2+} on the surface of the nanocomposite is most likely to be suitable complex formation between a non bonded electron in the amino-functionalized nanocomposite with Pb^{2+} and moreover the ~NH_2–Pb complex has high stability in the optimized natural pH.

$$Fe_3O_4@MCM\text{-}41\text{-}NH_2 + Pb^{2+} \rightarrow Fe_3O_4@MCM\text{-}41\text{-}NH_2\cdots\cdots Pb^{2+} \quad (4)$$

In subsequent Figs. (3D-F), at a constant pH, removal of Pb^{2+} enhanced by increasing in quantity of sorbent. This can be interpreted that available functional groups on the surface area of adsorbent to uptake ions from solution is too significant. As a final point, maximum removal was obtained when pH is about 7, the mass of adsorbent 0.01g, stirring time 3.5 min and lead ion concentration 15 $mg.L^{-1}$. At these conditions, maximum solute removal efficiency was obtained at 95.15 %.

Adsorption isotherm models

Equilibrium isotherm of the adsorbent for the removal of Pb^{+2} ions at the room temperature was studied by using Langmuir, Freundlich, Dubinin, and Radushkevich (D-R) and Timken isotherm models. The Langmuir isotherm model is predicted a monolayer coverage of the Pb(II) ions on the outer surface of the adsorbent. The Langmuir isotherm can be represented in linear form as follows:

The Langmuir equation is:

$$C_e/Q_e = 1/(K_L Q_{max}) + (1/Q_{max})C_e \quad (5)$$

Where Q_e ($mg.g^{-1}$) is the amount of solute adsorption at equilibrium, C_e ($mg.L^{-1}$) is the

Table 4. ANOVA for Response Surface Quadratic model

Source	Sum of Squares	df	Mean Square	F –Value	P-value	
Model	1168.20	14	83.44	50.28	< 0.0001	Significant
A-pH	70.73	1	70.73	42.62	< 0.0001	
B-adsorbent	423.87	1	423.87	255.42	< 0.0001	
C-Concentration	32.48	1	32.48	19.57	0.0005	
D-time	154.54	1	154.54	93.12	< 0.0001	
AB	0.042	1	0.042	0.025	0.8758	
AC	58.75	1	58.75	35.4	< 0.0001	
AD	0.76	1	0.76	0.46	0.5099	
BC	72.25	1	72.25	43.54	< 0.0001	
BD	1.58	1	1.58	0.95	0.3453	
CD	10.86	1	10.86	6.54	0.0219	
A^2	295.39	1	295.39	177.99	< 0.0001	
B^2	61.65	1	61.65	37.15	< 0.0001	
C^2	51.89	1	51.89	31.27	< 0.0001	
D^2	11.78	1	11.78	7.10	0.0177	
Residual	24.89	15	1.66			
Lack of Fit	19.97	10	2.00	2.03	0.2251	not significant
Pure Error	4.92	5	0.98			
Cor Total	1193.09	29				

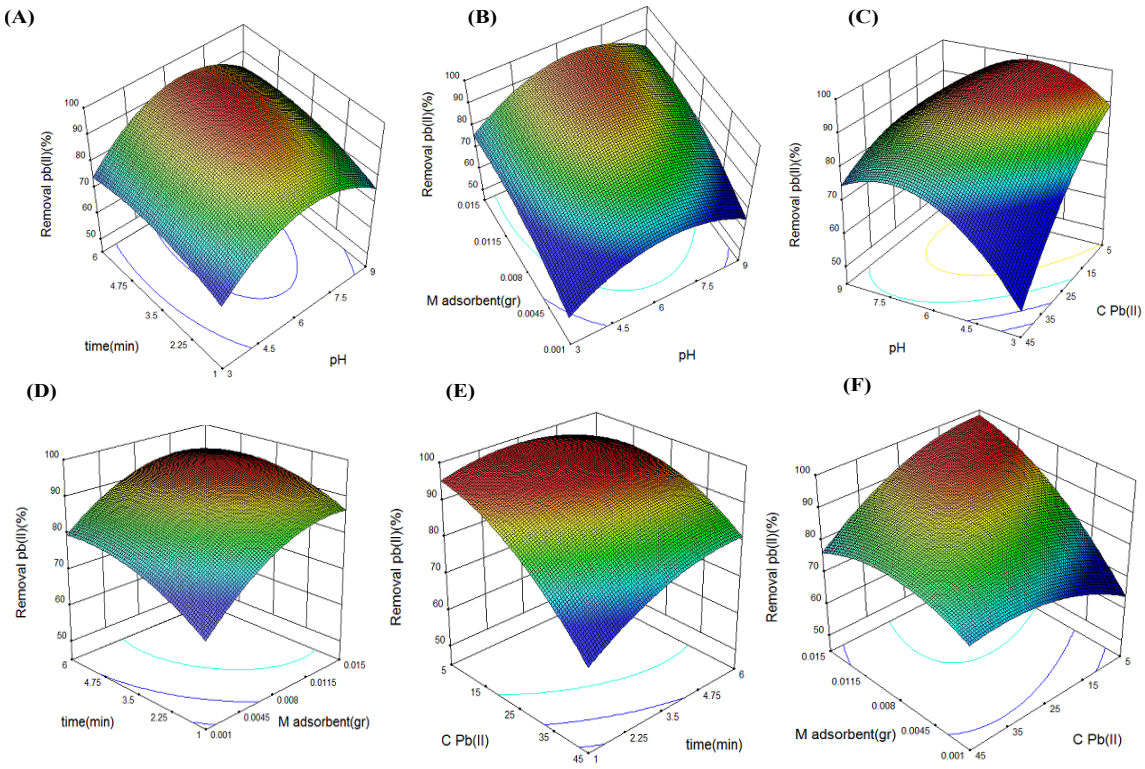

Fig. 3. The 3D surface plots for removal of Pb^{+2} ions. The response percent versus (A) the stirrer time and pH, (B) the amount of adsorbent and pH, (C) pH and the concentration of Pb^{+2} ions, (D) the stirrer time and the amount of adsorbent, (E) the concentration of Pb^{+2} ions and the stirrer time, (F) the amount of adsorbent and the concentration of Pb^{+2} ions

equilibrium concentration of solute, Q_m is the maximum monolayer of adsorbent ion capacity ($mg.g^{-1}$) and K_L($L.mg^{-1}$) is Langmuir constant. According to this equation, the C_e/ Qe has a linear correlation with C_e.

$$q_e=q_m bC_e/(1+bC_e) \quad (6)$$

A plot of $1/q_e$ versus $1/C_e$ should indicate a line with slope b(the Langmuir adsorption constant($L.mg^{-1}$) and intercept of q_m (theoretical maximum adsorption capacity($mg\ g^{-1}$)) [21].

Freundlich is another model that is an empirical equation and represents the adsorption heterogeneity surface. The linear for Freundlich isotherm is as follows:

$$Ln(q_e)=LnK_F+\frac{1}{n}\ LnC_e \quad (7)$$

K_F and n are Freundlich constants representing the capacity and intensity of the adsorption. The values of K_f and n were calculated from the slope and intercept of a linear plot of lnq_e versus lnC_e, respectively [22].

The Timken model gives information about the heat of adsorption and the adsorbent-adsorbate interaction. The linear equation of Temkin isotherm is given as:

$$q_e=B\ln K_T+B\ln C_e \quad (8)$$

Where B ($j.mol^{-1}$) is the Temkin constant and K_T ($L.mg^{-1}$)is the equilibrium binding constant.

In the Dobinin-Rodushkvich isotherm, the mean free energy of the adsorption (β) can be calculated which is related to chemical and physical of adsorption [23].

The linear form of D-R isotherm represented as:

$$\ln q_e=\ln q_s-\beta R^2T^2Ln\,(1+1/C)^2 \quad (9)$$

In this model, adsorption energy ($\beta\ mol^2(Kj^2)^{-1}$) and theoretical saturation capacity were calculated from the slope and the intercept of linear plot lnq_e vs. Ln $(1+1/C)\ )^2$ [24]. The obtained results are shown in Fig. 4.

Fitting the experimental data in isotherm models and the values of the parameters and their

related correlation coefficients are shown in Table 5. Freundlich isotherm with the highest value of correlation coefficients (R^2) can be used to explain the Pb^{+2} ions adsorption over magnetic nonporous.

Kinetic study

A kinetic study of adsorption is necessary as it gets information about how adsorption of a solute occurred on the adsorbent in aqueous solution. The mechanism of adsorption is related to the state of the adsorbent and the mass transport process. To examine the adsorption processes of Pb^{+2} ions on the adsorbent, several adsorption kinetic models such as pseudo-first-order [25], pseudo-second-order [26], intra-particle diffusion model [27] and Elovich model [28] were studied.

The pseudo-first order model was applied to fit the kinetic experimental data, which is expressed as:

$$\text{Log}(q_e-q_t) = \log q_e-(K_1 t)/2.303 \quad (10)$$

Where q_e ($mg.g^{-1}$) and q_t ($mg.g^{-1}$) are the

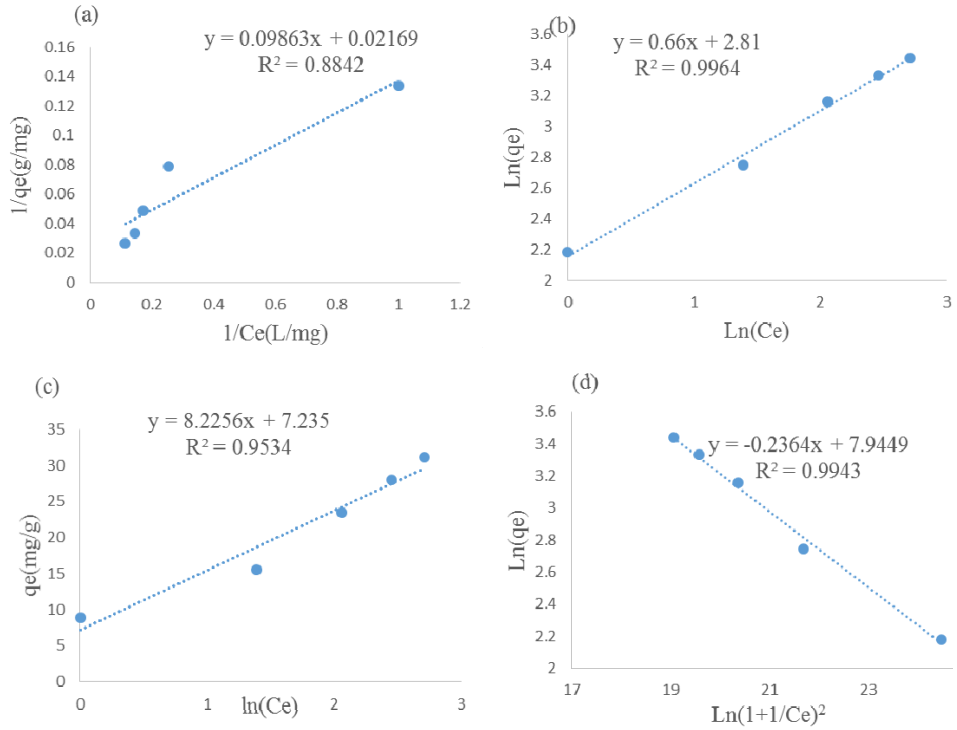

Fig. 4. Plots of isotherm models (a) Langmuir adsorption isotherm, (b) Freundlich adsorption isotherm, (c) Temkin adsorption isotherm and (d) Dobinin-Rodushkvich isotherm

Table 5. Isotherm constant parameters and correlation coefficients calculated for adsorption of Pb^{+2} onto Fe_3O_4@MCM-41-NH_2

Isotherm	Parameters	Value of parameter
Longmuir	q_m($mg.g^{-1}$)	46.08
	K_L($L.mg^{-1}$)	0. 22
	R^2	0.8842
Freundlich	1/n	1.55
	K_F($L.mg^{-1}$)	16.77
	R^2	0.9964
Temkin	K_T($L.mg^{-1}$)	2.41
	B_1	8.22
	R^2	0.9534
Dubinin-Radushkevich	q_s($mg.g^{-1}$)	2818.62
	E	3603.19
	$\beta \times 10^{-9}$	0.38
	R^2	0.9943

amount of solute that uptake by nanomagnetic at equilibrium and time t (min), respectively; and K_1 is the pseudo-first-order constant (min^{-1}).

The linearized integrate equation of the pseudo-second-order is given as:

$$t/q_t=1/(K_2q_e^2)+t/q_e \quad (11)$$

Scheming the values of t/q_t versus t gives a linear ship that from its slope and intercept, the values K_2 and q_e can be respectively determined.

The intra-particle diffusion model was used to describe several diffusion processes of the adsorbate from the bulk solution to the surface of the solid particles. The intra-particle diffusion model is generally expressed as:

$$q_t=K_{diff}\times t^{0.5}+C \quad (12)$$

Where q_t is the adsorption capacity at time t, K_{diff} is the intraparticle diffusion rate constant and C is the intercept that shows the boundary layer thickness.

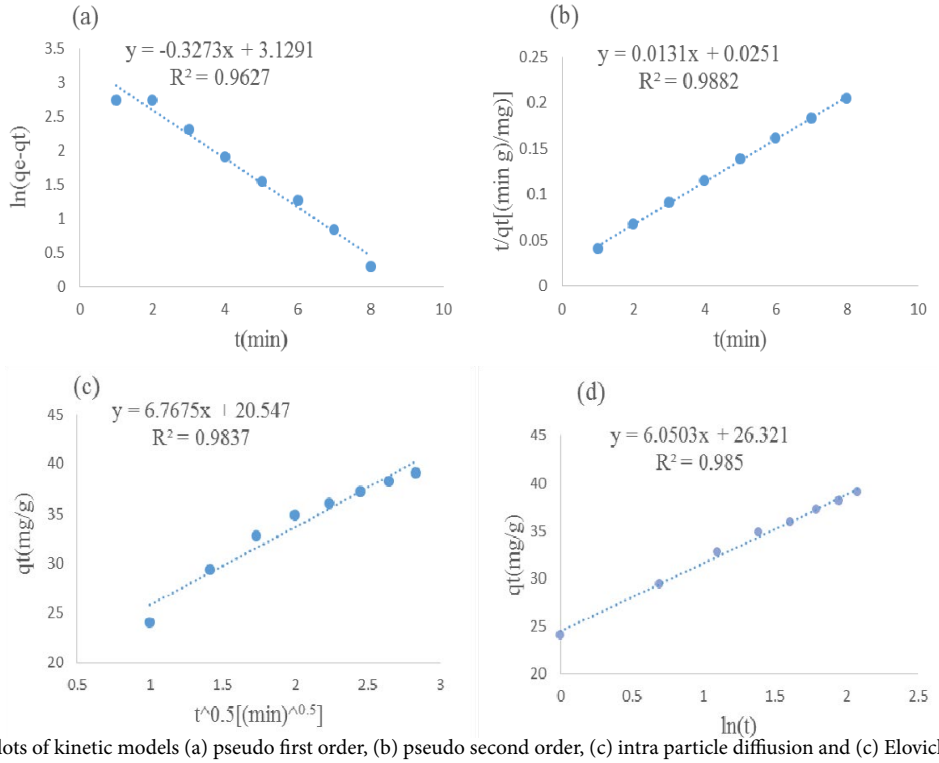

Fig. 5. Plots of kinetic models (a) pseudo first order, (b) pseudo second order, (c) intra particle diffiusion and (c) Elovich model

Table 6. Kinetic parameters for adsorption of Pb^{+2} ions by Fe_3O_4@MCM-41-NH_2

Model	Parameters	Pb^{+2} Concentration(ppm)		
		9	14	24
pseudo-first order kinetic	$k_1(min^{-1})$	0.3273	0.3285	0.4937
	$q_e(calc(mg.g^{-1}))$	22.850	25.115	38.860
	R^2	0.9627	0.949	0.9334
pesudeo-second-order kinetic	$k_2(min^{-1})$	0.0069	0.02142	0.017
	$q_e(calc(mg.g^{-1}))$	39.84	42.37	45.045
	R^2	0.9882	0.990	0.9948
Intra-partcle diffusion	$K_{diff}(mg.g^{-1}.min^{-1/2})$	6.7675	0.13	2.39
	R^2	0.9837	0.992	0.9708
Elovich	B	6.05	6.646	5.145
	A	0.21	5.10	0.249
	R^2	0.985	0.9515	0.8998
Experimental data	$q_e(exp)(mg.g^{-1})$	39.56	43.71	47.18

Table 7. Comparasion for the removal of lead by different adsorbent

Adsorbent	q_{max}	time(min)	Ref.
Fe_3O_4	52.90	1440	[29]
γ-Fe_2O_3	53.13	A few minute	[30]
Fe_3O_4-SO_3H	108.93	1440	[31]
Fe_3O_4@SiO2-EDTA	114.94	10	[32]
Fe_3O_4@MCM-41-NH_2	46.08	3.5	This work

The most helpful kinetics models to describe activated chemisorption on the surface of adsorbent is the Elovich equation. The linear form of the Elovich model is expressed by the following equation:

$$q_t = 1/\beta \ln(\alpha\beta) + 1/\beta \ln t \quad (13)$$

Where $1/\beta$ and $1/\beta \ln(\alpha\beta)$ obtained from the slope and the intercept of the plot of q_t vs. ln t. The results of these investigations are shown in Fig. 5. The best model was selected based on high-value linear correlation coefficient, R^2. As a result shown in Table 2, The pseudo-second-order model was the best model for fitting experimental data.

Comparison with other studies

The comparison between the present adsorbent and previously reported studies that reported in the literature regarding the removal time and maximum capacity of adsorption is shown in Table 7. It can be stated that in this study the proposed magnetite mesoporous in contrast with other reported adsorbents have a better or similar adsorption potential.

CONCLUSION

This study shows that Fe_3O_4@MCM-41-NH_2 was utilized for removal of Pb^{+2} ions from aqueous solutions. The efficiencies variables such as the amount of adsorbent, pH, contact time and concentration of Pb^{+2} were optimized using a central composite design. At optimum condition maximum efficiency removal 95.15 % were obtained. The adsorption processes followed pseudo-second-order kinetic model and equilibrium data fitted well in the Freundlich isotherm model with a correlation coefficient (0.9964). The value of maximum adsorption capacity, q_{max} was 46.08 for about 3.5 min.

ACKNOWLEDGMENTS

Authors appreciatively acknowledge the financial support of the University of Lorestan.

CONFLICTS OF INTEREST

The authors declare that there are no conflicts of interest.

REFERENCES

1. Brooks RM, Bahadory M, Tovia F, Rostami H. Removal of lead from contaminated water. International journal of soil, sediment and water. 2010;3(2):14.
2. Leusch A, Holan ZR, Volesky B. Biosorption of heavy metals (Cd, Cu, Ni, Pb, Zn) by chemically-reinforced biomass of marine algae. Journal of Chemical Technology AND Biotechnology. 1995;62(3):279-88.
3. Xu P, Zeng GM, Huang DL, Feng CL, Hu S, Zhao MH, et al. Use of iron oxide nanomaterials in wastewater treatment: A review. Science of The Total Environment. 2012;424:1-10.
4. Jalali R, Ghafourian H, Asef Y, Davarpanah S, Sepehr S. Removal and recovery of lead using nonliving biomass of marine algae. Journal of Hazardous Materials. 2002;92(3):253-62.
5. Iqbal M, Edyvean RGJ. Biosorption of lead, copper and zinc ions on loofa sponge immobilized biomass of Phanerochaete chrysosporium. Minerals Engineering. 2004;17(2):217-23.
6. Li X-m, Zheng W, Wang D-b, Yang Q, Cao J-b, Yue X, et al. Removal of Pb (II) from aqueous solutions by adsorption onto modified areca waste: Kinetic and thermodynamic studies. Desalination. 2010;258(1-3):148-53.
7. Quintelas C, Rocha Z, Silva B, Fonseca B, Figueiredo H, Tavares T. Removal of Cd(II), Cr(VI), Fe(III) and Ni(II) from aqueous solutions by an E. coli biofilm supported on kaolin. Chemical Engineering Journal. 2009;149(1-3):319-24.
8. Agrawal A, Sahu KK, Pandey BD. Removal of zinc from aqueous solutions using sea nodule residue. Colloids and Surfaces A: Physicochemical and Engineering Aspects. 2004;237(1-3):133-40.
9. Vukojević Medvidović N, Perić J, Trgo M, Mužek MN. Removal of lead ions by fixed bed of clinoptilolite – The effect of flow rate. Microporous and Mesoporous Materials. 2007;105(3):298-304.
10. González-Muñoz MJ, Rodríguez MA, Luque S, Álvarez JR. Recovery of heavy metals from metal industry waste waters by chemical precipitation and nanofiltration. Desalination. 2006;200(1-3):742-4.
11. Babel S, Kurniawan TA. Low-cost adsorbents for heavy metals uptake from contaminated water: a review. Journal of hazardous materials. 2003;97(1-3):219-243.
12. Baker HM, Massadeh AM, Younes HA. Natural Jordanian zeolite: removal of heavy metal ions from water samples using column and batch methods. Environmental Monitoring and Assessment. 2008;157(1-4):319-30.
13. Wang S, Wu H. Environmental-benign utilisation of fly ash as low-cost adsorbents. Journal of Hazardous Materials.

2006;136(3):482-501.
14. Zhou K, Yang Z, Liu Y, Kong X. Kinetics and equilibrium studies on biosorption of Pb(II) from aqueous solution by a novel biosorbent: Cyclosorus interruptus. Journal of Environmental Chemical Engineering. 2015;3(3):2219-28.
15. Selvam P, Bhatia SK, Sonwane CG. Recent Advances in Processing and Characterization of Periodic Mesoporous MCM-41 Silicate Molecular Sieves. Industrial & Engineering Chemistry Research. 2001;40(15):3237-61.
16. Liu J, Qiao SZ, Hu QH, Max Lu GQ. Magnetic Nanocomposites with Mesoporous Structures: Synthesis and Applications. Small. 2011;7(4):425-43.
17. Tahmasebi E, Yamini Y, Seidi S, Rezazadeh M. Extraction of three nitrophenols using polypyrrole-coated magnetic nanoparticles based on anion exchange process. Journal of Chromatography A. 2013;1314:15-23.
18. Stöber W, Fink A, Bohn E. Controlled growth of monodisperse silica spheres in the micron size range. Journal of Colloid and Interface Science. 1968;26(1):62-9.
19. Khaledyan E, Alizadeh K, Mansourpanah Y. Synthesis of Magnetic Nanocomposite Core–Shell Fe3O4@MCM-41-NH2 and its Application for Removal of Congo Red from Aqueous Solutions. Iranian Journal of Science and Technology, Transactions A: Science. 2018.
20. Javanbakht V, Ghoreishi SM. Application of response surface methodology for optimization of lead removal from an aqueous solution by a novel superparamagnetic nanocomposite. Adsorption Science & Technology. 2016;35(1-2):241-60.
21. Langmuir I. The Constitution and Fundamental Properties of Solids and Liquids. Part I. Solids. Journal of the American Chemical Society. 1916;38(11):2221-95.
22. Weber WJ, Morris JC. Kinetics of adsorption on carbon from solution. Journal of the Sanitary Engineering Division. 1963;89(2):31-60.
23. Ghaedi M, Ansari A, Habibi MH, Asghari AR. Removal of malachite green from aqueous solution by zinc oxide nanoparticle loaded on activated carbon: Kinetics and isotherm study. Journal of Industrial and Engineering Chemistry. 2014;20(1):17-28.
24. Dubinin MM, Serpinsky VV. Isotherm equation for water vapor adsorption by microporous carbonaceous adsorbents. Carbon. 1981;19(5):402-3.
25. Albadarin AB, Mangwandi C, Al-Muhtaseb AaH, Walker GM, Allen SJ, Ahmad MNM. Kinetic and thermodynamics of chromium ions adsorption onto low-cost dolomite adsorbent. Chemical Engineering Journal. 2012;179:193-202.
26. Shi L, Wei D, Ngo HH, Guo W, Du B, Wei Q. Application of anaerobic granular sludge for competitive biosorption of methylene blue and Pb(II): Fluorescence and response surface methodology. Bioresource Technology. 2015;194:297-304.
27. Ho YS, McKay G. Kinetic Models for the Sorption of Dye from Aqueous Solution by Wood. Process Safety and Environmental Protection. 1998;76(2):183-91.
28. Ghaedi M, Ghaedi AM, Negintaji E, Ansari A, Vafaei A, Rajabi M. Random forest model for removal of bromophenol blue using activated carbon obtained from Astragalus bisulcatus tree. Journal of Industrial and Engineering Chemistry. 2014;20(4):1793-803.
29. Rajput S, Pittman CU, Mohan D. Magnetic magnetite (Fe 3 O 4) nanoparticle synthesis and applications for lead (Pb 2+) and chromium (Cr 6+) removal from water. Journal of Colloid and Interface Science. 2016;468:334-46.
30. Rajput S, Singh LP, Pittman CU, Mohan D. Lead (Pb 2+) and copper (Cu 2+) remediation from water using superparamagnetic maghemite (γ-Fe 2 O 3) nanoparticles synthesized by Flame Spray Pyrolysis (FSP). Journal of Colloid and Interface Science. 2017;492:176-90.
31. Chen K, He J, Li Y, Cai X, Zhang K, Liu T, et al. Removal of cadmium and lead ions from water by sulfonated magnetic nanoparticle adsorbents. Journal of Colloid and Interface Science. 2017;494:307-16.
32. Liu Y, Fu R, Sun Y, Zhou X, Baig SA, Xu X. Multifunctional nanocomposites Fe 3 O 4 @SiO 2 -EDTA for Pb(II) and Cu(II) removal from aqueous solutions. Applied Surface Science. 2016;369:267-76.